BIM-CFD INTEGRATED SUSTAINABLE AND RESILIENT BUILDING DESIGN FOR NORTHERN ARCHITECTURE

Muna Younis[1], Meseret T. Kahsay[1], and Girma T. Bitsuamlak[1]
[1]Department of Civil and Environmental Engineering/Boundary Layer Wind Tunnel Laboratory/ WindEEE Research Institute, University of Western Ontario, ON, Canada

ABSTRACT

The buildings in northern Canada have unique climatic and environmental challenges, and therefore, the need for innovative building design has become a vital requirement in a sustainable and resilient future. This study proposes a framework to integrate building information modeling (BIM) and computational fluid dynamics (CFD) analysis to study microclimate effects on buildings. As an application an investigation of different case scenarios of building heights above ground $(0.5m, 1m, 1.5m, 2m)$, wind speeds $(5m/s, 7m/s, 9m/s)$, and wind directions $(0°, 45°, 90°)$ is presented here. Results reveal that building downwash effect is a key factor in heat transfer to ground and therefore raising it $1m$ above ground is recommended.

INTRODUCTION

Climate change represents serious environmental, social, and economic challenges for the Northwest Territories, including rapidly warming temperatures, sea ice change, and permafrost degradation (Grosse et al. 2011). If no action is taken to mitigate this phenomenon, the problem will likely continue and aggravated, leading to an increase in the level of carbon and methane in the atmosphere (IPCC 2013). These Northern communities, therefore, experience many concerns to sustain themselves. Many of the current houses are in poor quality and their design may have not considered harsh climate conditions in Northern Canada (*i.e.* 90% of the Nunavik population live in unsuitable houses). Further, a big number of these houses were built directly on the ground causing permafrost to thaw faster underneath. Thaw settlement affects ground stability (Fortier, LeBlanc, and Yu 2011) also requires an extra budget for the construction and maintenance process. Investigating convective heat transfer in the Northern climate is crucial to maintain the frozen state of the ground and prevent permafrost degradations. Uses of wind-tunnel and full-scale measurements are difficult due to time and cost constraints for low-rise buildings. The multiphysics nature of the problem is another challenge. Alternatively, the use of computational fluid dynamics (CFD) is considered in this study. CFD provides high-resolution numerical simulation that can model wind flow. As such, with the power of CFD, it is possible nowadays to perform a full-scale analysis and high Reynolds numbers $(Re = 10^5 - 10^7)$ rather than the traditional reduced-scale tests (Hanna et al. 2006). The integration of Building Information Modeling (BIM) with CFD also provides efficient workflows that help determine the outdoor environmental condition (Delavar et al. 2019). The BIM model is designed and saved as an exchangeable format that allows the data transformation with physical and functional characteristics of structures (Eastman et al. 2011; Younis, El Ansary, and Bitsuamlak 2018). Much work has been conducted in the related literature to investigate and monitor permafrost heat transport and evaluate the factors that can be related directly to increase the thawing on the ground surface. In this instance, different modules have been developed to study coupled heat and water transfer in the permafrost layer to provide insight into the interaction between shallow groundwater, warming permafrost, and permafrost thaw rates (Ge et al. 2011), (Bense et al. 2012), (McKenzie and Voss 2013), and (Kurylyk, MacQuarrie, and McKenzie 2014). Likewise, the impact of thermal advection was investigated using numerical models by (Wellman, Voss, and Walvoord 2013) on permafrost thawing. The authors reveal that thermal advection can significantly increase thawing rates. Other studies found that building facades contribute to a significant portion of heat losses, which can be obtained from the convective heat transfer (Palyvos 2008), and thereby these heat loss can change the thermal dynamics of permafrost. Authors (Gruber and Hoelzle 2008) remarked that air circulation driven by the temperature gradient between the air inside and outside buildings has not been treated sufficiently as most of the numerical simulations have not taken into consideration the influence of convective heat transfer in permafrost regions. Evaluating convective heat transfer coefficient (CHTC) of building facades is not a simple task as it strongly depends on the interaction between a wide range of parameters such as building geometry and surrounding, wind flow and speed, and surface roughness (Montazeri et al. 2015).

To our best knowledge, the relation between building heat losses and permafrost is not well studied. This paper presents high-resolution 3D BIM-CFD integrated simulations of CHTC on the building surfaces and the permafrost ground layer in the Arctic region. Particularly, it analyzes the variation of CHTC with building raised from the ground at different heights, subjected to different wind speeds, and wind directions of $(0.5m, 1m, 1.5m,$

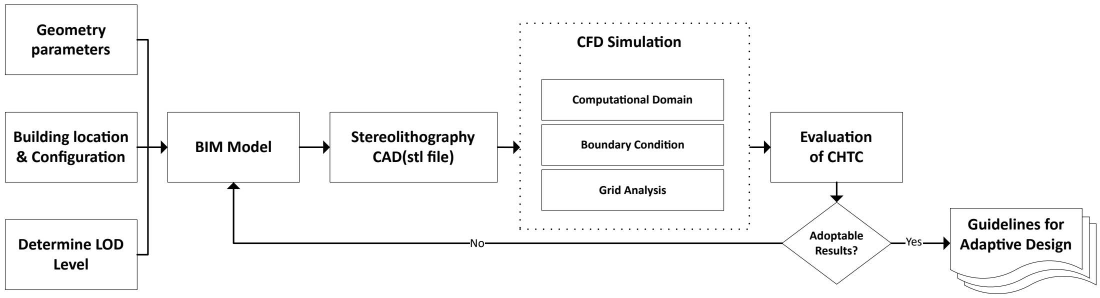

Figure 1: BIM-based CFD simulation

and $2m$), ($5m/s, 7m/s$, and $9m/s$), and ($0°, 45°$, and $90°$), respectively. Also, forced convection is considered only in this work as the relative importance of the buoyancy effect is negligible. This is due to the fact that the ratio of the Grashof number to the Reynolds numbers squared is small.

METHODOLOGY

The proposed BIM-supported framework is presented in this section. BIM is used as a tool for sustainable built environment that exchange and save the model information between 3D CAD and CFD software. The framework of the proposed approach is demonstrated in Figure 1. The first step in the proposed approach is to create a 3D BIM model with accurate building geometry, location, and level of details (LOD) which was 100 LOD as demonstrated in Figure 2. The geometry of the building used to represent the height, width, and length are $6m, 9.75m$, and $11m$ respectively. With the exported stl file from the BIM model, CFD and heat transfer simulation is carried out to evaluate CHTC variation of the building and permafrost as well as the flow field. The convective heat transfer is governed by Newtons law of cooling and can be calculated as shown in Equation 1

$$CHTC = \frac{q_c}{T_s - T_{ref}} \tag{1}$$

where CHTC is W/m^2K, q_c the convective heat flux density (W/m^2), T_s the surface temperature (K) and T_{ref} the reference temperature (K). The climate data of Iqaluit, Nunavut, Canada is used for the simulation. It is worth mentioning that this city is considered the main air transportation hub for the eastern Arctic. Winter weather conditions between Nov. to Feb. were chosen because of the expected high heat losses due to the high joint occurrence of the wind speed and temperature difference between inside and outside of buildings, which represents critical stressor for permafrost degradation.

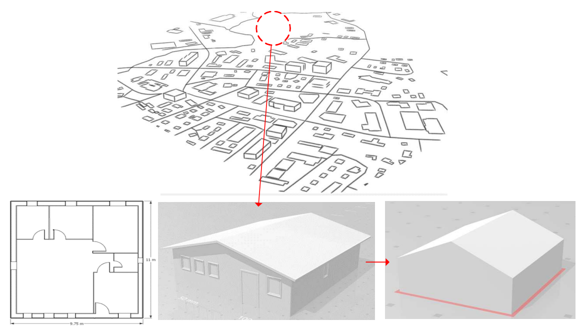

Figure 2: BIM built environment

CFD Simulations

As listed in Table 1, different scenarios have been simulated to evaluate the effect of each design parameter on building surfaces and permafrost ground. The 3D steady Reynolds-averaged NavierStokes (RANS) equation with the Shear stress turbulent (SST) $k-\omega$ closure model is used to model the turbulent wind flow and energy equation is solved to predict the CHTC. SST $k-\omega$ provides sufficient accuracy on building surfaces and able to capture flow characteristics near the wall (Kahsay, Bitsuamlak, and Tariku 2019). The authors reported their results of the CFD model validation in Figures 3 and 4. In their study, CFD simulation of a cube was performed to evaluate the surface temperature along a mid-height horizontal centerline and a mid-plan vertical line. They also compared their work with other studies including experimental data presented by (Meinders, Hanjalic, and Martinuzzi 1999) and CFD simulations reported by (Montazeri et al. 2015; Defraeye, Blocken, and Carmeliet 2010). The simulations produced accurate CHTC predictions for the windward surface utilizing the two-equation SST $k-\omega$ model. Based on the CFD validation from literature, the same set of parameters has been adopted in this study. As such, commercial CFD solver STAR-CCM+ and SHARCNET high-performance computing at Western University has been used to perform the simulation process.

Table 1: Simulation scenarios & design parameters

Ground height (m)	Wind speeds (m/s)	Wind direction
0.5	5, 7, 9	0°
1	5, 7, 9	0°
1	7	45°
1	7	90°
1.5	5, 7, 9	0°
2	5, 7, 9	0°

* Ground height represents distance above the ground

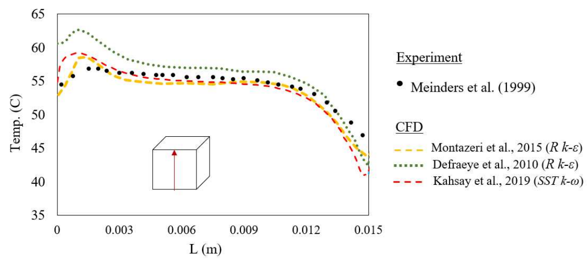

Figure 3: Comparison of experimental measured and simulated temperature distribution on the windward surfaces of the cube in horizontal center plane (Kahsay, Bitsuamlak, and Tariku 2019)

Computational domain

Figure 5 shows the computational domain (CD) extends $5H$ upstream, $15H$ downstream of the building, and $5H$ height based on the practice guidelines discussed in (Dagnew and Bitsuamlak 2014; Franke et al. 2011), where H denotes for building height. More precisely, these guidelines show that the CD dimensions allow the atmospheric boundary layer (ABL) profile interaction details upstream and wake flow redevelopment downstream.

Boundary conditions

In this study, three different wind speeds of $U_{10} = 5m/s, 7m/s$, and $9m/s$ were used at the reference height of $10m$. logarithmic law assumed to describe the ABL at inlet of CD, see Equation 2. The mathematical calculation of Turbulent kinetic energy $K(m^2/s^2)$ and turbulence dissipation rate $\varepsilon(m^2/s^3)$ are shown in Equation 3 and 4, respectively. Detailed explanations about these inflow boundary conditions are provided in (Richards and Norris 2011).

$$U(z) = \frac{U_*}{k} ln\left(\frac{z+z_0}{z_0}\right) \tag{2}$$

$$K = 3.3u_*^2 \tag{3}$$

$$\varepsilon = \frac{U_*^3}{k(z+z_0)} \tag{4}$$

The parameters of these profiles allow to produce a neutral ABL, where the friction and shear are the main source of turbulence generation, u_* is friction velocity (m/s), z_0 is the aerodynamic roughness length $z_0 = 0.03m$ (Emes et al. 2017) (ESDU 2001), and k is the von Karman constant (~ 0.42). A uniform inlet air temperature of $T_{ref} = 248$K is selected based on the winter weather data of Iqaluit city (Ghias et al. 2017; GOC 2019). The temperature of the building surfaces is constant and fixed to $T_w = 303$K, while the ground surface is assumed to be a constant temperature boundary condition with a value of $T_g = 259$K (Oldenborger and LeBlanc 2015; GNWT 2014). The top and lateral sides of the domain are considered symmetry boundary conditions.

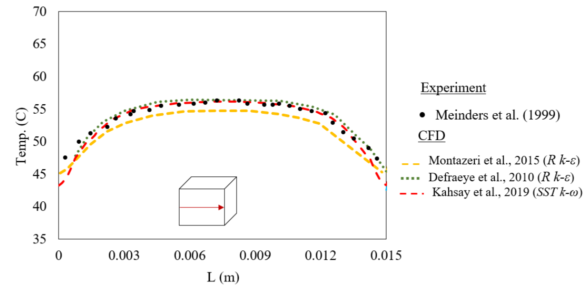

Figure 4: Comparison of experimental measured and simulated temperature distribution on the windward surfaces of the cube in vertical center plane (Kahsay, Bitsuamlak, and Tariku 2019)

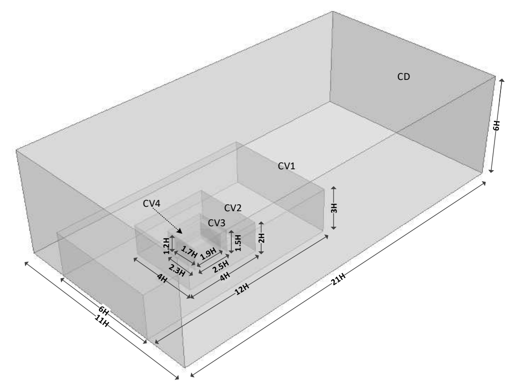

Figure 5: Computational domain-perspective view

Grid dependency analysis

To perform the grid dependency analysis, a CHTC of the windward surface is compared for G1 (coarse), G2 (medium) and G3 (fine) to ensure the optimum mesh size. Figure 6 shows the three levels of grid density with grid 1 (3150000 cells), grid 2 (5150000 cells), and grid 3 (6200000 cells). The simulated CHTC result does not change significantly between grid 2 & 3, see Figure 7. Therefore, the finest grid (3) distribution has been adopted in the present study. Convergence is assumed when all the scaled residuals level off and reach the values 10^{-7} for x, y, z-momentum, energy, continuity, and k and ε.

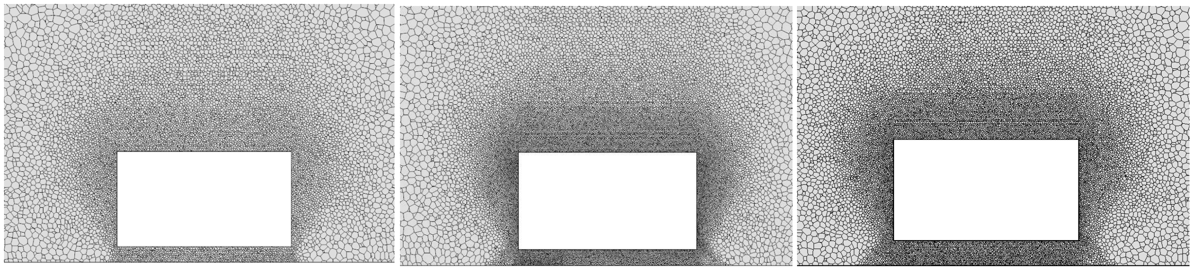

(i) Grid 1 (ii) Grid 2 (iii) Grid 3

Figure 6: Grids comparison

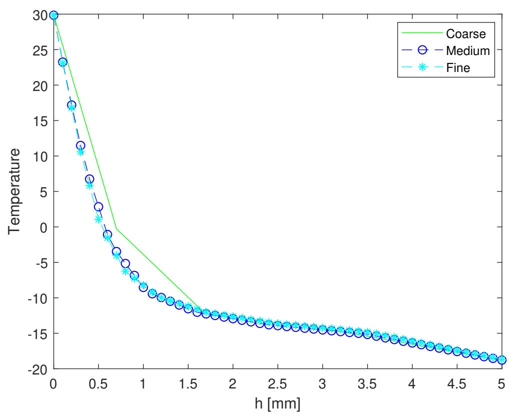

Figure 7: Grid sensitivity analysis

The computational domain with its four control volumes (CV1, CV2, CV3, and CV4) are depicted in Figure 5. Each sub-domain represents a different mesh size with a refined grid near the building's exterior surfaces. To achieve a high-resolution grid near the building surfaces in CV4 (finest mesh) , fine grids are deployed to obtain small $y^+ < 5$ to capture essential details of the temperature gradients near the walls. Equation 5 shows the mathematical expression of y^+.

$$y^+ = \frac{u_* y}{\nu} \tag{5}$$

where y is the distance to the nearest wall, ν is the local kinematic viscosity. To increase the accuracy of the mesh, 10 prism layers at the viscous boundary layer are generated on the building surfaces with a total thickness of 2.1mm (Figure 8). The value of 1.05 is selected for the stretching factor to get better grid clustering properties that able to resolve the boundary layer at all solid-fluid interfaces of CV4. As recommend by (Kahsay, Bitsuamlak, and Tariku 2019), the first cell spacing should be between the range 120μm and 150μm for accurate CHTC analysis. The mesh setup in this work has a minimum distance from building surfaces of 150μm, which located within the recommended range.

RESULTS AND DISCUSSIONS

In this study, building height, wind velocity, and wind direction parameters were investigated to determine their impacts on the Northern building architecture and permafrost ground underneath. Different simulated scenarios were performed and the results of selected scenarios are administrated in Figure 9. It can be clearly seen in all scenarios that high-temperature gradient between building surfaces (303K) and the outside air (248K) leads to ascending air in the surrounding area. It is worth mentioning that, building surface temperature value was taken as recommended in the related literature by (Blocken et al. 2009; Kahsay, Bitsuamlak, and Tariku 2019). Thus, this convective air circulation causes temperature distribution and heat transfer between the whole system.

Scenarios 1,2,3, & 4, study the impact of different building heights of ($0.5m, 1m, 1.5m$, and $2m$) above the ground, while the wind speed and direction are $7m/s$ and $0°$, respectively. In the first scenario as shown in Figure 9 (i)-c&d, when building raised above the ground 0.5m, the airflow underneath is accelerated within a narrow strip in yellow and red colors, while the red color indicates to high CHTC values. Therefore, the 0.5m is not sufficient to reduce the heat transfer from the building to the permafrost. It is worth mentioning that, the shadow area under the buildings' frame is often expected to be the highest CHTC values in permafrost ground. Hence, such areas should be excluded from the pilings foundation and screwjacks implementation. In contrast, better results observed in terms of reducing thermal effect on permafrost when the building is raised 1m above the ground as shown in Figure 9 (ii)-c&d. This can be justified when the open space between the building and permafrost ground increased, the heat losses dissipate by free circulation of the air. Likewise, Figures 9 (iii and iv)-c&d show better results in comparison with the first two scenarios in mitigating the building downwash effect, as well as reduces the intensity of convective air circulation over the strip region as shown in scenario 1. Also, these two simulations identify the contribution of the redevelopment of the circulation in

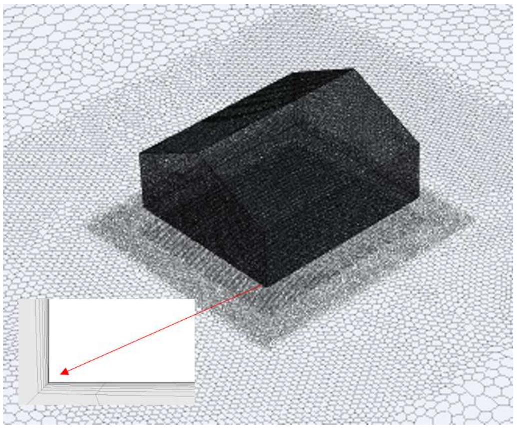

Figure 8: Prism layers distribution

the wake area and its role in redistributing the heat over the surrounding area. Among the previously discussed scenarios, a positive correlation has been noticed between raising the building above the ground and reducing the thermal stress on permafrost. In light of such a scenario, this demonstrates that permafrost is extremely sensitive to thermal changes. Despite the yielded promising results from raising the building of reducing thermal stresses on permafrost, the CHTC distribution on windward surface has increased as demonstrated in Figure 9 (i, ii,iii, & iv)-a. These results show a positive correlation between height and CHTC values.

Extremely strong winds represent one of the climate characteristics in the Northern region. Thus, additional simulations are performed to obtain correlations of the forced CHTC with wind speed for windward surface and permafrost ground, see Figures 9 (ii, v, and vi)-b&c. According to the figures, it has been noticed that when the wind velocity is increased, the CHTC values for both building surfaces and permafrost ground are increased as well. Due to the intensity of the air circulation, more rate of convective heat transfer is occurring between the building and the permafrost layer. Figure 11 demonstrates a comparison of surface-averaged CHTC of windward face with different wind velocities of $(5, 7,$ and $9m/s)$ and heights $(0, 0.5, 1, 1.5,$ and $2m)$. The results reflect a significant impact of wind speed on CHTC; when the velocity increased from $5m/s$ to $9m/s$, the surface-averaged CHTC has increased on the windward face by 43.2%. The CHTC also has the highest values on the building edges due to the air separation at the sharp edges. Accordingly, it is recommended to install proper insulation at these locations to reduce heat losses from the building surfaces and heat transfer to the permafrost.

This study also evaluates the effect of wind directions on permafrost by comparing wind approaching from angles 45° and 90°. As Figure 10-(i & ii) depicts, when the

Table 2: Correlation of surface-averaged CHTC & wind direction

Wind angle	CHTC	Deference (%)
0°	27.94	-
45°	24.89	11.6 %
90°	21.19	27.2 %

wind approach from angles 45°, the intensity of wind will be distributed over two faces. This, in turn, reduces the CHTC values by 11.6% on the windward face in comparison with the 0°. Similarly, when the wind approaching the building from angle 90° , the heat transfer and CHTC of the windward face reduced by 27.2%. Table 2 shows the correlation of CHTC and wind direction for $1m$ elevated building.

Over the total simulations of 22 scenarios, it has been noted that elevated buildings above the ground have two contradictory effects. More precisely, having an open space underneath the building obtain encouraging results for preserving the frozen state of permafrost. Nonetheless, such a solution increases CHTC on the windward face causing more heat losses. A strong correlation also has been observed between the CHTC and wind velocities. Based on the obtained results, it is recommended to raise the building above the ground by $1m$ in the Northern climate. This selection can be justified by the fact that among all heights, the $1m$ height has yielded better results (intermediate) in both permafrost ground and CHTC of the windward face. Considering the above-mentioned advantages, the $1m$ represents a reasonable and convenient height for elderly people. Further, to mitigate the wind speed's negative impact, building orientation and form should be taken into consideration in the designing of Northern buildings.

CONCLUSION

This study focused on the Northern climate which is uniquely sensitive to the climate change impacts such as rapidly warming temperatures, sea ice change, and permafrost degradation. While much of the infrastructure in this region relies on the properties of permafrost frozen state for stability, heat transfer from structures causes ground warming leads to permafrost degradation. Typically, the proposed solution to overcome such a problem is to raise the building above the ground to create an open space underneath prevents wind drifted snow accumulation and reduces the thermal stress on the permafrost. The current study quantified the impact of raising buildings from ground $(0.5m, 1m, 1.5m, 2m)$, wind speeds $(5m/s, 7m/s, 9m/s)$, and wind directions $(0°, 45°, 90°)$. Some of the observations include:

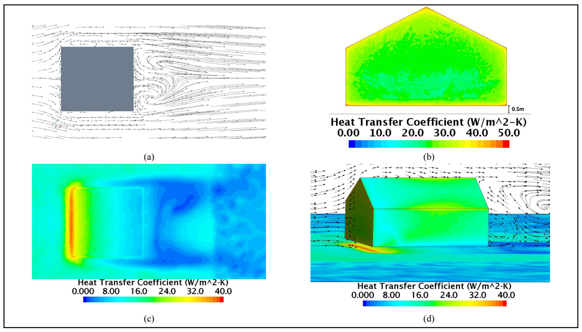

(i) Scenario 1: $h = 0.5m, V = 7m/s, 0^{\circ}$

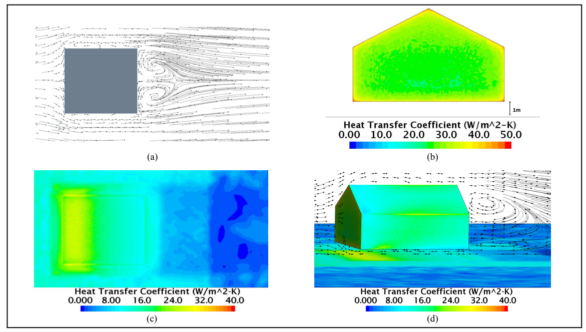

(ii) Scenario 2: $h = 1m, V = 7m/s, 0^{\circ}$

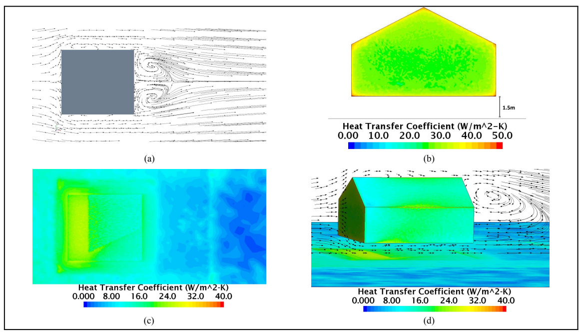

(iii) Scenario 3: $h = 1.5m, V = 7m/s, 0^{\circ}$

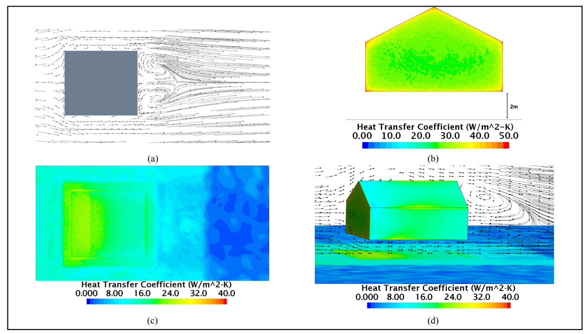

(iv) Scenario 4: $h = 2m, V = 7m/s, 0^{\circ}$

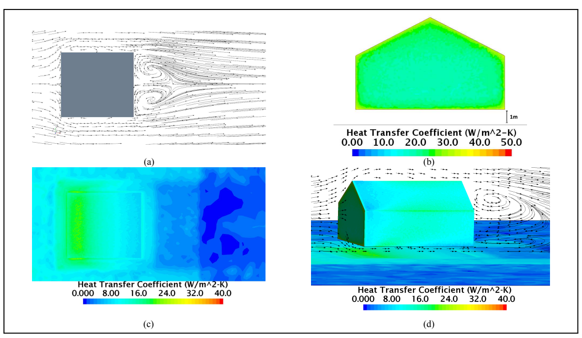

(v) Scenario 5: $h = 1m, V = 5m/s, 0^{\circ}$

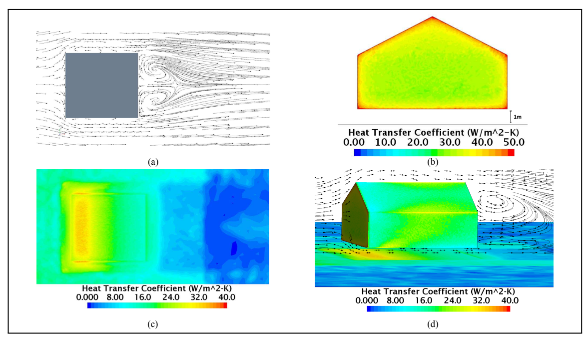

(vi) Scenario 6: $h = 1m, V = 9m/s, 0^{\circ}$

Figure 9: Comparison of CHTC among selected raised building scenarios

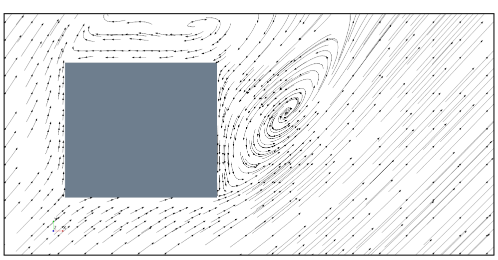

(i) Velocity contours plan at 4m. Scenario 7: $h = 1.5m, V = 7m/s, 45^{\circ}$

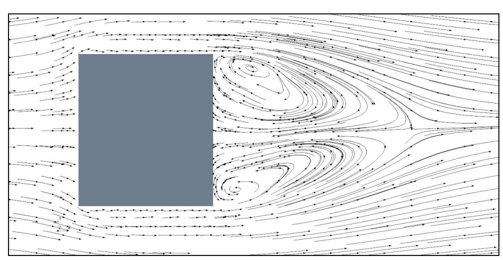

(ii) Velocity contours plan at 4m. Scenario 7: $h = 1.5m, V = 7m/s, 90^{\circ}$

Figure 10: Velocity contours

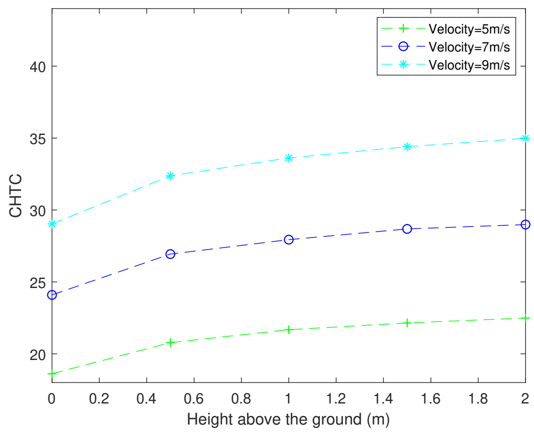

Figure 11: Surface-averaged CHTC comparison for windward face

1. Permafrost is sensitive to the height of the building above the ground. A building height of $1m$ above ground shows most suitable for the Northern climatic as it reduces the thermal stresses on the permafrost.

2. Avoid pilings foundation and screwjacks implementation in the shadow area under the buildings' frame since it is exposed to the highest heat transfer. Note that for permafrost regions, these two methods are imperfect solutions as thawing ground can disrupt the structure.

3. Uses special insulation in buildings edges and corners not only to enhance the energy saving, but also to reduce the heat transfer enormously from building to the permafrost underneath.

4. Building orientation should be considered in the early design stages to alleviate building downwash effect on permafrost ground.

In summary, under the Northern climate, wind speeds and directions are a leading factor affecting permafrost thaw through downwash effect, which in turn transfers the heat from building surfaces to ground. The building height above the ground also significantly affects heat transfer to the permafrost layer. The study also provides a better understanding of the building-permafrost relation, as well as suggests adaption strategies for this unique climate.

ACKNOWLEDGMENT

The authors would like to acknowledge SHARCNET for providing access to their high performance computation facility and excellent support from their technical staff.

NOMENCLATURE

T_{ref}	reference air temperature (K)
$u(z)$	mean wind speed
u_*	friction velocity (m/s)
z	*a* reference height
z_0	aerodynamic dynamic roughness length
ε	turbulence dissipation rate (m^2/s^3)

REFERENCES

Bense, V. F., H. Kooi, G. Ferguson, and T. Read. 2012. "Permafrost degradation as a control on hydrogeological regime shifts in a warming climate." *Journal of Geophysical Research: Earth Surface* 117, no. F3.

Blocken, B., T. Defraeye, D. Derome, and J. Carmeliet. 2009. "High-resolution CFD simulations for forced convective heat transfer coefficients at the facade of a low-rise building." *Building and Environment* 44 (12): 2396 – 2412.

Dagnew, Agerneh K, and Girma T Bitsuamlak. 2014. "Computational evaluation of wind loads on a standard tall building using LES." *Wind and Structures* 18 (5): 567–598.

Defraeye, Thijs, Bert Blocken, and Jan Carmeliet. 2010. "CFD analysis of convective heat transfer at the surfaces of a cube immersed in a turbulent boundary layer." *International Journal of Heat and Mass Transfer* 53 (1): 297 – 308.

Delavar, Mohammad, Girma T Bitsuamlak, John K Dickinson, and Leandro Malveira F Costa. 2019. "Automated BIM-based process for wind engineering design collaboration." *Building Simulation*. Springer, 1–18.

Eastman, Chuck, Paul Teicholz, Rafael Sacks, and Kathleen Liston. 2011. *BIM handbook: A guide to building information modeling for owners, managers, designers, engineers and contractors*. John Wiley & Sons.

Emes, Matthew J., Maziar Arjomandi, Farzin Ghanadi, and Richard M. Kelso. 2017. "Effect of turbulence characteristics in the atmospheric surface layer on the peak wind loads on heliostats in stow position." *Solar Energy* 157:284 – 297.

ESDU, IHS. 2001. "Characteristics of Atmospheric Turbulence Near the GroundPart II: Single Point Data for Strong Winds (Neutral Atmosphere)." *Engineering Sciences Data Unit, IHS Inc., London, UK, Report No. ESDU*, vol. 85020.

Fortier, Richard, Anne-Marie LeBlanc, and Wenbing Yu. 2011. "Impacts of permafrost degradation on a road embankment at Umiujaq in Nunavik (Quebec), Canada." *Canadian Geotechnical Journal* 48 (5): 720–740.

Franke, Jorg, Antti Hellsten, K. Heinke Schlunzen, and Bertrand Carissimo. 2011. "The COST 732 Best Practice Guideline for CFD simulation of flows in the urban environment: a summary." *International Journal of Environment and Pollution* 44 (1-4): 419–427.

Ge, Shemin, Jeffrey McKenzie, Clifford Voss, and Qingbai Wu. 2011. "Exchange of groundwater and surface-water mediated by permafrost response to seasonal and long term air temperature variation." *Geophysical Research Letters* 38, no. 14.

Ghias, Masoumeh Shojae, René Therrien, John Molson, and Jean-Michel Lemieux. 2017. "Controls on permafrost thaw in a coupled groundwater-flow and heat-transport system: Iqaluit Airport, Nunavut, Canada." *Hydrogeology journal* 25 (3): 657–673.

GNWT. 2014. Ground temperature in permafrost zones. `https://www.enr.gov.nt.ca/en/state-environment/131-ground-temperature-permafrost-zones`.

GOC. 2019. Daily Data Report. `https://climate.weather.gc.ca`.

Grosse, Guido, Vladimir Romanovsky, Torre Jorgenson, Katey Walter Anthony, Jerry Brown, and Pier Paul Overduin. 2011. "Vulnerability and Feedbacks of Permafrost to Climate Change." *Eos, Transactions American Geophysical Union* 92 (9): 73–74.

Gruber, Stephan, and Martin Hoelzle. 2008. "The cooling effect of coarse blocks revisited: a modeling study of a purely conductive mechanism." *9th International Conference on Permafrost*. Institute of Northern Engineering, University of Alaska Fairbanks, 557–561.

Hanna, Steven R., Michael J. Brown, Fernando E. Camelli, Stevens T. Chan, William J. Coirier, Olav R. Hansen, Alan H. Huber, Sura Kim, and R. Michael Reynolds. 2006. "Detailed Simulations of Atmospheric Flow and Dispersion in Downtown Manhattan: An Application of Five Computational Fluid Dynamics Models." *Bulletin of the American Meteorological Society* 87 (12): 1713–1726.

IPCC, Climate Change. 2013. "The Physical Science Basis In: Stocker TF, Qin D, Plattner GK, Tignor MMB, Allen SK, Boschung J, et al., editors." *Fifth Assessment Report of the Intergovernmental Panel on Climate Change. Cambridge, UK: Cambridge University Press*, p. 1535.

Kahsay, Meseret T, Girma T Bitsuamlak, and Fitsum Tariku. 2019. "CFD simulation of external CHTC on a high-rise building with and without façade appurtenances." *Building and Environment* 165:106350.

Kurylyk, Barret L., Kerry T.B. MacQuarrie, and Jeffrey M. McKenzie. 2014. "Climate change impacts on groundwater and soil temperatures in cold and temperate regions: Implications, mathematical theory, and emerging simulation tools." *Earth-Science Reviews* 138:313 – 334.

McKenzie, Jeffrey M, and Clifford I Voss. 2013. "Permafrost thaw in a nested groundwater-flow system." *Hydrogeology Journal* 21 (1): 299–316.

Meinders, E. R., K. Hanjalic, and R. J. Martinuzzi. 1999. "Experimental Study of the Local Convection Heat Transfer From a Wall-Mounted Cube in Turbulent Channel Flow." *Journal of Heat Transfer* 121 (3): 564–573 (08).

Montazeri, H., B. Blocken, D. Derome, J. Carmeliet, and J.L.M. Hensen. 2015. "CFD analysis of forced convective heat transfer coefficients at windward building facades: Influence of building geometry." *Journal of Wind Engineering and Industrial Aerodynamics* 146:102 – 116.

Oldenborger, Greg A., and Anne-Marie LeBlanc. 2015. "Geophysical characterization of permafrost terrain at Iqaluit International Airport, Nunavut." *Journal of Applied Geophysics* 123:36 – 49.

Palyvos, J.A. 2008. "A survey of wind convection coefficient correlations for building envelope energy systems modeling." *Applied Thermal Engineering* 28 (8): 801 – 808.

Richards, P.J., and S.E. Norris. 2011. "Appropriate boundary conditions for computational wind engineering models revisited." *Journal of Wind Engineering and Industrial Aerodynamics* 99 (4): 257 – 266. The Fifth International Symposium on Computational Wind Engineering.

Wellman, Tristan P, Clifford I Voss, and Michelle A Walvoord. 2013. "Impacts of climate, lake size, and supra-and sub-permafrost groundwater flow on lake-talik evolution, Yukon Flats, Alaska (USA)." *Hydrogeology journal* 21 (1): 281–298.

Younis, Muna, Ayman El Ansary, and Girma Bitsuamlak. 2018. "Sustainable building design in cold climate region: A framework for residential building." *Annual Conference of the Canadian Society for Civil Engineering*. CSCE Fredericton, Canada.